The End of a 30-Year-Old Controversy? A Computational Study of the B−N Stretching Frequency of BH_3−NH_3 in the Solid State

Jan Dillen* and Paul Verhoeven

Department of Chemistry, University of Stellenbosch, Private Bag X1, Matieland 7602, South Africa

Received: October 18, 2002; In Final Form: January 31, 2003

The molecular geometry and vibrational frequencies of borane ammoniate, BH_3−NH_3, are studied by ab initio calculations in the solid state. The B−N bond distance shortens by ∼0.08 Å, and the corresponding stretching frequency increases by 200 cm^{-1}, compared to the same characteristics of the molecule in the gas phase. A reassignment of the experimental argon-matrix vibrational spectrum in an earlier work [Smith, J.; Seshadri, K. S.; White, D. *J. Mol. Spectr.* **1973**, *45*, 327−337], on the basis of these calculations, unifies all the experimental vibrational data available for this molecule. The shortening of the B−N bond is analyzed in terms of the atoms-in-molecules theory.

Introduction

The molecular structure of borane ammoniate, BH_3−NH_3, and similar donor−acceptor complexes continues to be of considerable interest. A common feature of these complexes is that the B−N bond, or, generally, the bond between the donor atom and the acceptor atom, is considerably shorter in the crystal than it is in the gas phase. In BH_3−NH_3, for example, the B−N bond length is found[1] via microwave spectroscopy to be equal to 1.6722(5) Å (r_o value, r_s = 1.658(2) Å). Two early X-ray diffraction (XRD) studies[2,3] at room temperature (space group *I*4*mm*, disordered) indicate much shorter distances (1.56(5) and 1.6(2) Å). Below 220 K, the molecule crystallizes in an orthorhombic space group; the B−N bond length is found to be 1.564(6) Å via XRD[4] and 1.58(2) Å using a recent neutron diffraction study.[5]

The IR and Raman spectra of BH_3−NH_3 and several isotope-substituted species in liquid ammonia and dimethyl ether have been reported by Taylor et al.,[6−8] with special emphasis on the value of the B−N stretching frequency, which was established to be 787 cm^{-1}. Taylor also mentioned that, in dimethyl ether, this value is lower by ∼40 cm^{-1}. Vibrational spectra of several compounds of the form X_3B−NR_3, including BH_3−NH_3 and some of its isotope-substituted species, were measured in the solid state by Sawodny et al.[9] They also carried out a normal coordinate analysis, confirming the B−N stretching frequency to be in the same region at 776 cm^{-1}. These results are in sharp contrast to an argon-matrix study by Smith et al.,[10] who assign this normal mode to 968 cm^{-1}, a value that is also supported by a normal coordinate analysis involving deuterated species.

On the computational side, several ab initio studies have focused on the molecular geometry, binding energy, topology of the electron density, and vibrational frequencies of BH_3−NH_3.[11−23] Using self-consistent reaction field (SCRF) calculations, Schleyer et al.[13] calculated that, with hexane as a solvent, the B−N bond length is reduced from 1.689 Å for the isolated molecule to 1.62 Å in solution. In water, it would be 1.57 Å. On the basis of these results, it was suggested that the dipolar field could be responsible for the observed shortening of the dative bond in the crystal. In another ab initio study, Frenking et al.[15] used a simple dimer and tetramer model of antiparallel molecules to simulate the solid-state structure of BH_3−NH_3. From these results, it was proposed that short-range dipole−dipole interactions between the molecules are responsible for the significant shortening of the bond.

The majority of computational studies that mention the calculation of vibrational frequencies of BH_3−NH_3 quote the experimental B−N stretching value of 968 cm^{-1}, determined by Smith et al.,[10] and conclude from the observed discrepancy between experiment and calculations that explicit or implicit introduction of electron correlation is essential to calculate the properties of this molecule. A comprehensive study by Vijay et al.,[17] however, employing large basis sets and high levels of theory, rejected the above-mentioned value, in favor of Taylor's result of 785 cm^{-1}. The authors also commented that the systematic underperformance of the various calculated results was contrary to "general observations". Indeed, very often, the calculated frequencies are multiplied by an empirical scale factor. The recommended scale factor for a HF/6-31G(d) calculation, which is used in this study, for example, is 0.8929.[27] This factor reduces the already-low calculated B−N stretch frequency of 604 cm^{-1} to 538 cm^{-1}.

In this paper, we present a detailed computational study of the structural and vibrational properties of crystalline BH_3−NH_3. Our intent was to investigate, in more detail, the geometrical differences that exist between the molecule in the solid state and in the gas phase; the corresponding changes that occur in the vibrational frequencies also are investigated.

Computational Details

Calculations were performed with the Gaussian 98 program[24] at the self-consistent field (SCF) and Møller−Plesset second-order (MP2) levels of theory and the standard 6-31G(d) basis set. The crystal environment of BH_3−NH_3 was simulated by surrounding one single molecule with several neighbors, as shown in Figure 1. Coordinates for the atoms were generated from the experimental neutron diffraction data of Klooster et al.[5] Only the central molecule was allowed to adjust its position during the energy minimization, and the molecule was constrained to lie on the crystallographic mirror plane. The

* To whom correspondence should be addressed. Author can be contacted via E-mail (E-mail address: jlmd@sun.ac.za).

10.1021/jp027240g CCC: $25.00
Published on Web 03/13/2003

coordinates of all the atoms of the surrounding molecules were fixed to the experimental values. The latter are determined by neutron diffraction, so the positions of the H atoms are well established. Geometrical optimizations on the isolated molecule and the molecular clusters shown in Figure 3 were carried out under the molecular point-group symmetry of each system.

Vibrational frequencies were calculated within the harmonic approximation from a mass-weighted, analytical second-derivative matrix. Vibrational normal modes were visualized and characterized with an updated version of the program Vibram.[25] The analysis of the electron density in terms of the atoms-in-molecules (AIM) theory[26] was performed with the AIMPAC suite of computer programs, as supplied by Bader's research group. The programs were modified to handle larger systems but were otherwise used unaltered.

Results and Discussion

The various models used to represent the crystal phase are shown in Figure 1. In these models, the number of molecules is progressively increased, mainly in the direction of the molecular axis, to give clusters with 8 (model **1**), 10 (model **2**), 18 (model **3**), and 20 (model **4**) surrounding molecules. In addition, model **3** was also extended in the other two spatial directions to give model **5**, with 30 molecules around the central BH_3−NH_3. These clusters of semiparallel displaced dipoles closely mimic the experimental geometry found in the crystal.

As is evident from Table 1, the B−N bond progressively shortens as the size of the computational crystal increases. The effect is very large, even for the smaller models, e.g., going from a length of 1.689 Å for the isolated molecule to 1.653 Å for **1** and 1.625 Å for **2**. This confirms the suggestion by Frenking et al.[15] that short-range interactions could be mainly responsible for this effect. A further, but less pronounced, decrease is noticed for the larger models **3** and **4**. However, the increase of the bond length in **5** to 1.623 Å, compared to the value of 1.611 Å in **3**, suggests that long-range interactions cannot be ignored and, in fact, do play an important role. Because of the large computational effort, only **1** was calculated at the MP2 level. However, the results confirm the trend observed with the Hartree−Fock (HF) calculation, i.e., a shortening of the B−N bond in the crystal environment.

Another interesting aspect is the observation that the charge distribution in the molecule changes considerably as a function of the number of surrounding molecules. This is illustrated most comprehensively by comparing the total charge of the NH_3 group in the various models, with the charge of the BH_3 group being equal in size but opposite in sign. The charge on the NH_3 group in the isolated molecule is +0.262 e. This value decreases slightly to +0.254 e in **1** and increases progressively in magnitude to +0.328 e in **4**. This corresponds to a 25% loss of negative charge that flows to the BH_3 group. In **5**, which differs from **1**−**4** by the addition of molecules in the other two spatial directions, the charge decreases again.

This redistribution of charge—and, hence, electron density—is also evident in the Laplacian (second derivative) of the electron density, which is shown for the mirror plane bisecting the molecule in Figure 2. There is a noticeable broadening of the area covered by the solid lines; this broadening represents a local increase in electron density near the location of the critical point of the B−N bond, compared to that of the isolated molecule. Numerical values that support this observation are also given in Table 1. It is seen that the electron density at the bond critical point (BCP), $\rho_b(r)$, changes from 0.088 au for the isolated molecule to 0.116 au in **4**, an increase of 32%. Despite the shortening of the bond when going from **1** to **4**, the relative position of the BCP remains situated at ~69% of the B−N bond length from the N atom.

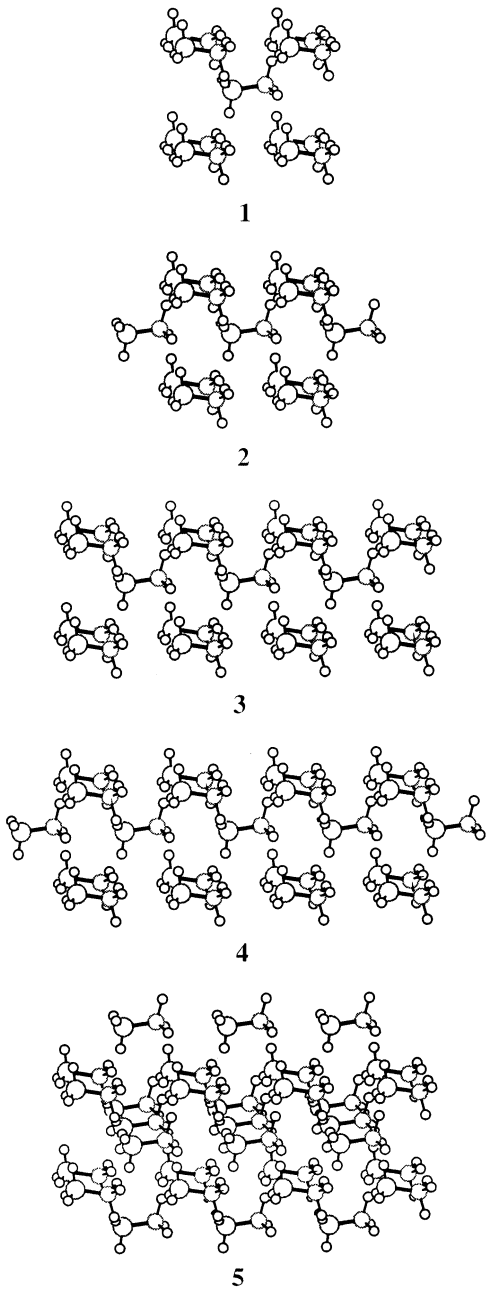

Figure 1. Models used to simulate the crystal environment. Experimental and fixed coordinates are used for all molecules, except the central one, whose position was optimized (see text).

TABLE 1: Selected Calculated Properties of BH_3−NH_3 in the Gas Phase and in the Solid State

model	r(B−N), Å	q(NH_3), e	$\rho_b(r)^a$	$-\nabla^2\rho_b(r)^b$
		HF Level		
gas	1.689	0.262	0.088	0.523
1	1.653	0.254	0.098	0.564
2	1.625	0.298	0.109	0.579
3	1.611	0.323	0.115	0.571
4	1.609	0.328	0.116	0.569
5	1.623	0.303		
		MP2 Level		
gas	1.664	0.273		
1	1.635	0.259		

[a] In units of e·(Bohr)$^{-3}$. [b] In units of e·(Bohr)$^{-5}$.

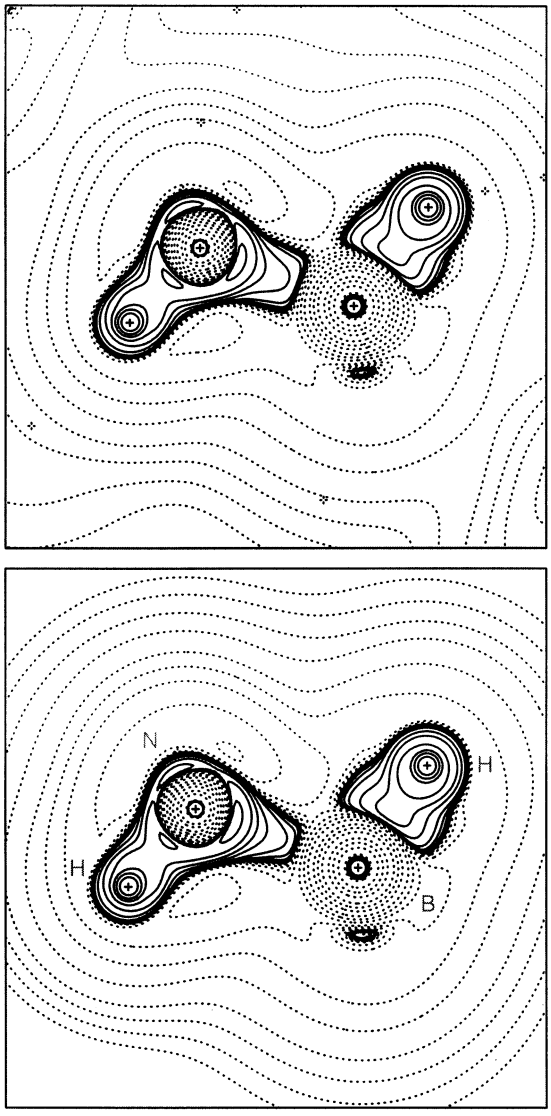

Figure 2. Laplacian of the electron density (top, central BH_3-NH_3 in crystal model **4**; bottom, isolated BH_3-NH_3 molecule). Dashed lines show areas of electron depletion ($\nabla^2\rho(r) > 0$), whereas solid lines show areas of electron concentration ($\nabla^2\rho(r) < 0$).

The existence of a N−H···H−B dihydrogen bond in crystalline BH_3-NH_3 has been proven experimentally with the neutron diffraction study on this molecule[5] and has also been studied computationally on a dimer model within the context of the AIM theory by Popelier.[21] We were able to locate the BCPs between all the H atoms involved in the formation of the dihydrogen bonds; however, the data did not reveal much dependency on the size of the crystal used in the calculation. The electron density at the BCP of N−H decreases by <1%, compared to that of the isolated molecule, and by ∼3% for the B−H bond. The calculated values of the shortest H···H distance of 2.03 Å in **1** down to 2.00 Å in **4** are in good agreement with the experimental value of 2.02(3) Å. No noticeable lengthening of either the N−H or B−H bonds is observed in the calculated crystals, which is in agreement with the small changes in electron density at the BCP. The values of the electron density and its Laplacian at the BCPs are all similar to those reported by Popelier and, therefore, will not be discussed any further.

As stated previously, one of the major purposes of this work was to resolve the differences between the various experimental assignments of the B−N stretching frequency. Because of the dramatic shortening of this bond in the solid state as calculated with **1**−**5**, a noticeable shift in the calculated stretching frequency is to be expected.

TABLE 2: Calculated (Unscaled) Vibrational Frequencies[a]

mode	gas	**1**	**2**	**3**
		A_2 Symmetry		
torsion	253	212	214	211
		374	371	367
		A_1 Symmetry		
B−N str	604	684	760	798
BH_3 def	1280	1259	1283	1289
NH_3 def	1484	1488	1541	1578
B−H str	2560	2560	2561	2544
N−H str	3691	3706	3711	3704
		E Symmetry		
NH_3 rock	681	751−752	768−778	779−789
BH_3 rock	1132	1164−1167	1181−1183	1185−1189
BH_3 def	1294	1302−1357	1303−1363	1307−1367
NH_3 def	1838	1822−1838	1826−1844	1825−1845
B−H str	2604	2642−2671	2618−2640	2592−2607
N−H str	3816	3835−3842	3830−3836	3815−3821

[a] All values given in units of cm^{-1}.

However, calculating this property poses some difficulties. First, there is the computational effort. Because of limitations of the available computational resources, only the vibrational frequencies of **1**−**3** could be calculated at the HF level. Another complication is the fact that the coordinates of all the surrounding molecules are kept fixed during the energy minimization. This results in a large number of negative (actually imaginary) frequencies that—through coupling—may influence the "genuine" normal modes of the central molecule in an adverse way. Fortunately, visual inspection (by animation) of the normal modes allows clear and unambiguous identification of most normal modes, except for the rocking vibrations; the results are given in Table 2. A range of frequencies is given for some of the normal modes, because the degeneracy is lifted due to coupling with the surrounding molecules. The two rocking modes are highly correlated, and the distinction between an NH_3 rock and a BH_3 rock is motivated by the observed frequency shifts of the deuterated species discussed later. Even in the small model **1**, the B−N stretching frequency increases from 604 cm^{-1} to 684 cm^{-1}, climbing further to 798 cm^{-1} in **3**. Assuming that the recommended scale factor[27] of 0.8929 for a HF/6-31G(d) calculation mentioned previously is valid for all the systems studied here, this observation implies that the calculated frequency in the isolated molecule is only 539 cm^{-1}, increasing to 713 cm^{-1} in **3**. Although this value is still ∼60−70 cm^{-1} short of the experimental values of Sawodny et al.[9] and Taylor et al.,[6−8] this figure represents a significant improvement from previous computational results.[12,17,18,22] Bearing in mind that the experimental B−N bond distance is 1.58(2) Å, or ∼0.02 Å shorter than that obtained with any of our models, we anticipate that the use of, for example, a MP2 level of theory would further improve the correspondence between the calculations and experiment. The results also indicate that a B−N stretching frequency of 968 cm^{-1}, as proposed by Smith et al.,[10] seems very unlikely.

A full list of the scaled calculated vibrational modes, together with their description, and a comparison with the matrix, liquid, and solid-state spectra are given in Table 3. As can be seen from this table, two frequencies that are heavily influenced by the crystal environment—in addition to the B−N stretch—are the symmetric NH_3 deformation and the NH_3 rocking mode. To a lesser extent, the BH_3 rocking and asymmetric deformation modes are also affected. Overall, the calculated frequencies are in good agreement with the assignment as proposed by Sawodny

TABLE 3: Calculated[a] Vibrational Frequencies for BH_3−NH_3 Compared to Existing Experimental Data with Proposed New Assignment

	calculated				experimental					
	gas		crystal (model **3**)		argon matrix[b]		KBr/Nujol[c]		liquid NH_3[d]	
mode	$^{11}B/^{10}B$	int[e]	^{11}B	int[e]	org[f]	new[g]	org[f]	new[g]	org[f]	new[g]
					A_2 Symmetry					
torsion	226	0	188 + 328[h]	65 + 10	n.o.[i]		n.o.[i]		n.o.[i]	
					A_1 Symmetry					
B−N str	539/553	35	713	21	968/987	603 (n.o.[i]?)	776/790		787	
BH_3 def	1143/1149	174	1151	106	1052/1060		1026	1058	1175	1060
NH_3 def	1325	181	1409	131	1343	1301	1374		1060	1175?
B−H str	2286/2288	88	2272	191	2340		2277		2285	
N−H str	3296	14	3307	56	3337		3245		3183	
					E Symmetry					
NH_3 rock	608	2	696−704	1−3	1301	n.o.[i] (603?)	715		n.o.[i]	
BH_3 rock	1011/1017	55	1058−1062	59−79	603	968/987	1058	1026	n.o.[i]	1026
BH_3 def	1155/1159	16	1167−1221	9−29	1186		1165		1026	n.o.[i]
NH_3 def	1641	36	1630−1647	20−32	1608		1597		1600	
B−H str	2325/2338	322	2314−2328	250−346	2415/2427		2316		2316	
N−H str	3407	42	3406−3412	115−145	3386		3312		3309	

[a] Scaled by 0.8929. All values in table given in units of cm^{-1}. [b] Reference 10. [c] Reference 9. [d] References 6−8. [e] Calculated intensity (km/mol). [f] Original assignment. [g] New assignment (if different from the original assignment). [h] See text for explanation. [i] Not observed.

et al.[9] Their spectra are measured using KBr pellets and Nujol samples, which imply crystalline BH_3−NH_3, and these results can thus be compared directly with our calculations. The largest deviation between the calculations and the experiment is for the calculated value of 1151 cm^{-1} for the symmetric BH_3 deformation. An alternative would be to assign Sawodny's experimental value of 1058 cm^{-1} to this mode and 1026 cm^{-1} to the BH_3 rock. This assignment results in a small improvement only but could be more appropriate if the calculated intensity of the peaks is taken into consideration. Taylor assigned a value of 1175 cm^{-1} to the BH_3 (A_1) deformation mode, which is in good agreement with the calculations; however, the peak at 1060 cm^{-1} that Taylor assigned to the NH_3 (A_1) deformation mode is too low, according to the calculations.

The vibrational spectrum of a matrix-isolated substance is supposed to resemble the spectrum of the isolated molecule closely, because the technique involves the trapping of a molecule at cryogenic temperatures in an excess of inert material. However, the same factors that contribute to solvent effects—e.g., inductive, electrostatic, and dispersive interactions, but also the rigidity of the matrix cage—may contribute to significant shifts of the vibrational absorption frequencies. A typical example is the monomer IR spectrum of HCl,[28] which displays large bathochromic wavenumber shifts, depending on the matrix material used. To investigate the possibility of matrix effects with argon, we have performed calculations on two simple matrix models by embedding a single BH_3−NH_3 molecule into a cluster of 14 and 26 Ar atoms, respectively, and performing a full geometry optimization, followed by a calculation of vibrational frequencies. Although limited in size, these models are certainly adequate enough to model short-range interactions, if any, but the B−N stretching frequency increased only from 604 cm^{-1} to 608 and 609 cm^{-1}, respectively.

We therefore tried to rationalize the experimental matrix spectrum of BH_3−NH_3 in terms of a reassignment of the experimental spectrum to the computational data, the results of which are also summarized in Table 3. The major discrepancy between our assignment and that of Smith et al. is that we assign the peaks at 968/987 cm^{-1} to the BH_3 rocking mode, rather than to the B−N stretching frequency. This implies that the latter must be assigned to the observed value of 603 cm^{-1}, which, in view of the calculations, is not unreasonable, or it must be considered to be unobserved. Smith et al.[10] assigned this peak to the BH_3 rocking mode. They also assigned the peak at 1301 cm^{-1} to the NH_3 rocking mode, which, according to the calculations, should be ∼700 cm^{-1}. This peak is labeled as "very strong" in the experimental spectrum, and we believe that, also considering the calculated intensity, an assignment to the symmetric NH_3 deformation is more appropriate. This leaves the experimental peak at 1343 cm^{-1} unassigned.

A proposed reassignment of the experimental frequencies of the two deuterated species studied by Smith et al.[10] is given in Table 4. In the new assignment for BH_3−ND_3, all strong peaks are accommodated; the major change again is that the 945/960 cm^{-1} peaks are assigned to the BH_3 rocking mode. The results for the fully deuterated species are also given in this table. Admittedly, there are still some unresolved issues: it remains unclear, for example, why no B−N stretching frequency would have been observed in the fully deuterated product or why the reassigned ND_3 rocking mode at 466 cm^{-1} was measured only for this species. Sawodny et al.[9] did not observe this mode either, but they did report a peak at 574 cm^{-1}, which they assigned to the BD_3 rock. Although we did not calculate any deuterated species in the crystal, if it is assumed that the frequency shifts between the isolated molecule and the solid state for the deuterated compounds are similar to those of the parent BH_3−NH_3, the calculated value of the ND_3 rock should increase to ∼545 cm^{-1}, which is similar to Sawodny's observed value. Nevertheless, and considering the contamination of the experimental sample of BD_3−ND_3, some of the new assignments should be considered to be speculative, at best.

It is also noteworthy that, according to the calculations in the solid state, the torsional frequency (which is inactive in both the IR and Raman spectra) splits into two distinct peaks, at 118 and 328 cm^{-1}, representing separate rotational movements of the NH_3 and BH_3 groups, respectively. Penner et al.[29] have established the activation energies for rotation of these groups in the orthorhombic (ordered) crystal by deuterium NMR studies to be 13.7(0.9) and 26.4(1.4) kJ/mol. The quantitative agreement between these results and the calculated frequencies and the experimental activation energies is very poor; however, the same trend is obtained.

We have also performed some geometry optimizations and frequency calculations of BH_3−NH_3 in solution using the

TABLE 4: Calculated[a] and Experimental Vibrational Frequencies of Two Isotopomers of BH_3-NH_3

$^{11}BH_3-ND_3/^{10}BH_3-ND_3$				$^{11}BD_3-ND_3/^{10}BD_3-ND_3$			
	calc	org[b]	new[c]		calc	org[b]	new[c]
			A_1 Symmetry				
B−N str	518/531	945/960	610	B−N str	503/513	931/956	n.o.[d]
BH_3 def	1143/1150	1031/1040		BD_3 def	862/872	818	898/912
ND_3 def	1012	1100	1001	ND_3 def	1014	1038	1006
B−H str	2285/2287	2339		B−D str	1628/1630	1682	
N−D str	2359	2397		N−D str	2358	2406	
			E Symmetry				
ND_3 rock	484	1001	n.o.[d]	ND_3 rock	437	1006	466
BH_3 rock	952/959	610	945/960	BD_3 rock	774/776	466	818?
BH_3 def	1154/1157	1187		BD_3 def	854/862	898	870
ND_3 def	1189/1207	1271		ND_3 def	1188	1179	
B−H str	2325/2338	2414/2426		B−D str	1737/1755	1817/1837	
N−D str	2513	2528		N−D str	2513	2528	

[a] Scaled by 0.8929. All values given in units of cm^{-1}. [b] Original assignment taken from ref 10. [c] New proposed assignment (if different from the original assignment). [d] Not observed.

TABLE 5: B−N Bond Distance (r(B−N)), Dipole Moment, Charge on the Ammonia Group (q(NH_3)), and Vibrational Frequencies of BH_3-NH_3 in Solution, as a Function of the Dielectric Constant ϵ, Calculated Using the Onsager Solvation Model and a Cavity with Radius a_o = 3.36 Å

				vibrational frequency, cm^{-1}											
ϵ	r(B−N), Å	dipole moment, D	q(NH_3), e	A_2-tors	A_1-BN str	A_1-BH_3 def	A_1-NH_3 def	A_1-BH str	A_1-NH str	E-NH_3 rock	E-BH_3 rock	E-BH_3 def	E-NH_3 def	E-BH str	E-NH str
1.0	1.689	5.572	0.262	253	604	1279	1484	2560	3691	681	1132	1294	1838	2604	3816
1.3	1.684	5.677	0.269	253	615	1280	1493	2556	3690	686	1134	1294	1838	2597	3813
1.5	1.682	5.730	0.272	252	621	1280	1499	2553	3689	689	1135	1295	1838	2593	3811
2.0	1.678	5.829	0.279	252	631	1281	1507	2550	3688	693	1137	1296	1838	2586	3809
2.5	1.675	5.896	0.283	251	637	1281	1512	2547	3687	696	1138	1296	1838	2581	3807
3	1.673	5.945	0.286	251	642	1281	1517	2545	3687	697	1138	1297	1838	2577	3805
4	1.671	6.011	0.291	250	648	1281	1522	2542	3686	700	1139	1297	1838	2572	3803
6	1.668	6.083	0.297	250	655	1281	1528	2539	3685	703	1139	1298	1838	2567	3801
8	1.667	6.122	0.298	249	658	1281	1531	2537	3684	704	1140	1298	1838	2564	3800
10	1.666	6.147	0.300	249	660	1281	1533	2536	3684	705	1141	1298	1838	2562	3799
20	1.664	6.198	0.303	248	664	1281	1536	2533	3683	707	1141	1299	1838	2558	3797
50	1.663	6.230	0.305	248	667	1281	1539	2532	3683	708	1141	1299	1838	2555	3796
100	1.663	6.241	0.306	248	668	1281	1540	2532	3682	709	1141	1299	1838	2554	3796
200	1.663	6.247	0.306	248	669	1281	1540	2531	3682	709	1141	1299	1838	2554	3796

Onsager solvent model.[30] Schleyer et al.[14] have reported a dramatic shortening of the B−N bond in solution, using the more sophisticated polarized continuum model,[31] but did not calculate vibrational frequencies. A summary of our results, calculated with a cavity radius of a_0 = 3.36 Å, as determined by the Gaussian program on the isolated molecule, is given in Table 5. It is noted that, as the dielectric constant, ϵ, of the solvent increases, the B−N bond distance shortens and the dipole moment increases, as reported by Schleyer et al.;[14] however, the magnitude of the changes is much smaller. As was observed in our calculations on the crystal, the positive charge on the NH_3 group increases, contributing to the change in dipole moment. Similarly, the B−N stretching and NH_3 (A_1) deformation frequencies are the most affected. The calculations also predict a reduction in the N−H and B−H stretching frequencies, especially the latter; however, this effect is only partially observed in the solid-state calculations. Nevertheless, the calculations confirm the proposal made by Schleyer et al.[14] that the crystal field has the same effect on the properties of BH_3-NH_3 as the dipole field of the solvent. Thus, in the absence of any other solvent effects, the vibrational spectrum of the molecule in solution should be similar to the solid-state spectrum. These results could also explain the observation made by Taylor that the B−N stretching frequency in dimethyl ether (ϵ = 6.2, −15 °C) is less than that in liquid ammonia (ϵ = 16.6).[32] At its melting point, the ϵ value of solid argon is 1.6,[33] which would have only a small effect on the B−N stretch.

We also tested Frenking's proposal[15] that short-range dipole−dipole interactions are responsible for the shortening of the B−N bond, by performing calculations on a wider variety of dimers, trimers, and higher molecular aggregates, shown in Figure 3. In Frenking's dimer, the two molecular dipoles are arranged in an antiparallel fashion, and in the tetramer, the central molecule faces the direction opposite that of the three surrounding molecules. In terms of dipole−dipole interactions, this arrangement is very stable, although different than that found in the crystal. We therefore wanted to test whether this stability could translate to an even shorter B−N bond distance, and possibly higher stretching frequency, than in the solid state. Although it is unlikely that BH_3-NH_3 would form large aggregates in the gas phase (and, thus, also in the argon matrix), the existence of dihydrogen bonds could, in principle, result in the formation of, for example, dimers and trimers and, hence, influence the vibrational spectrum of the molecule in a low-temperature matrix study.

Dimers. Crabtree et al.[34] used the PCI-80/B3LYP method to study five different models, four of which were found to be energy minima. The lowest dimer was found to have C_2 symmetry. Frenking's dimer has C_{2h} symmetry with both HF and MP2 calculations and a 6-31G(d) basis set. We have confirmed the latter result; however, we also found that models with the lower C_i and C_2 symmetry all converge to the same final structure but the Gaussian 98 package, despite the most-stringent convergence criteria, reports the lower symmetry. The

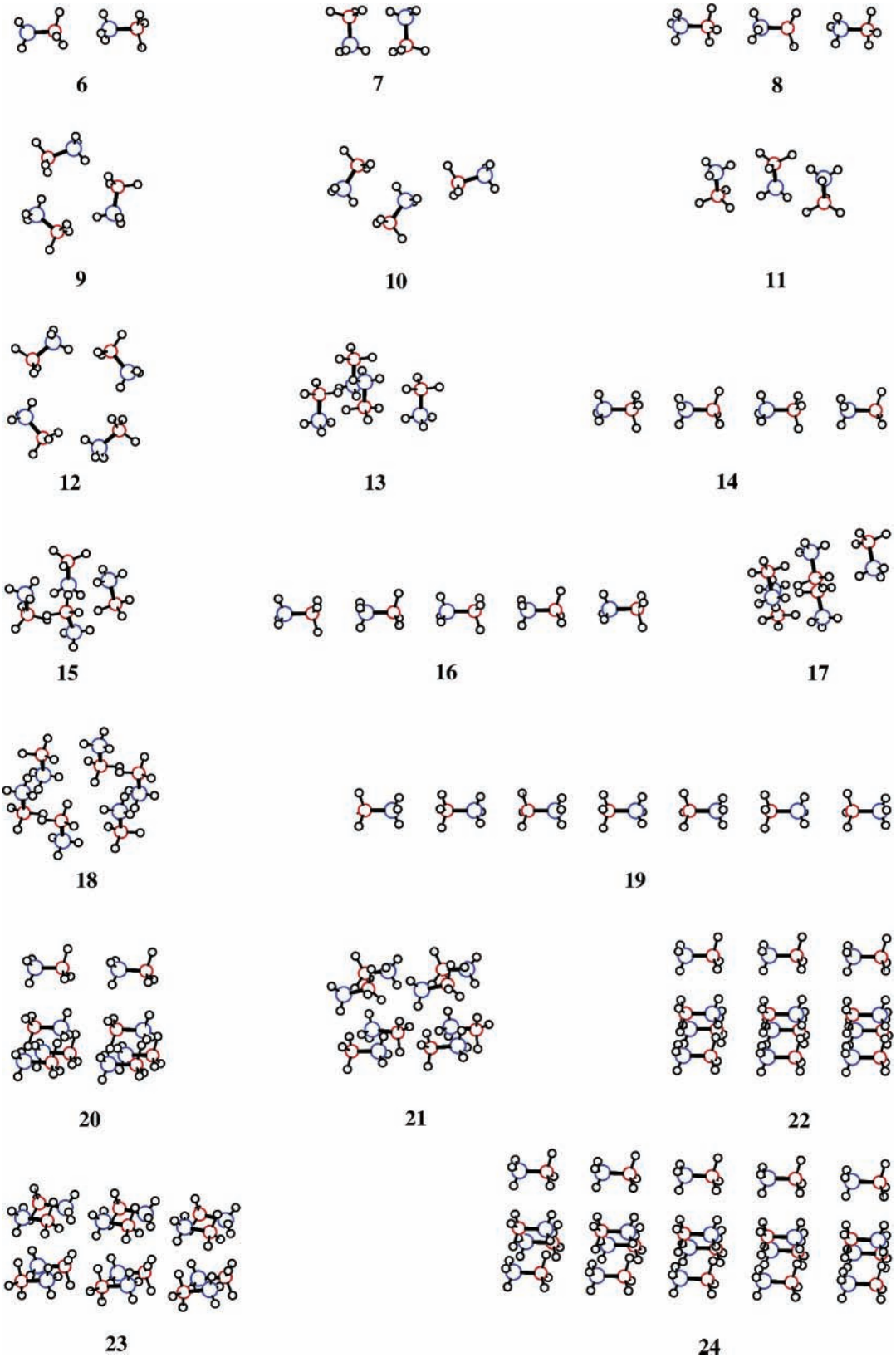

Figure 3. Schematic view of the molecular clusters studied. Nitrogen atoms are colored blue.

B−N bond in this dimer, **7**, is 1.659 Å, with a stretching frequency (unscaled) of 676 cm^{-1}. The higher-energy dimer **6** has bond lengths of 1.669 and 1.666 Å, with corresponding lower frequencies.

Trimers. Four stable trimers were found, of which the C_{3h} form **9** is the most stable. It features a B−N bond length of 1.647 Å and a stretching frequency of 708 cm^{-1}. The central molecule in the C_s form **11** has a bond length of 1.639 Å and a stretching frequency of 729 cm^{-1}.

Of the four stable tetramers found, the S_4 form **15** has the lowest energy. By virtue of its symmetry, all B−N bonds are equal at 1.648 Å, exhibiting a stretching frequency of 703 cm^{-1}. The central molecule in Frenking's tetramer **13** has a very short B−N bond, only 1.622 Å, and a corresponding stretching

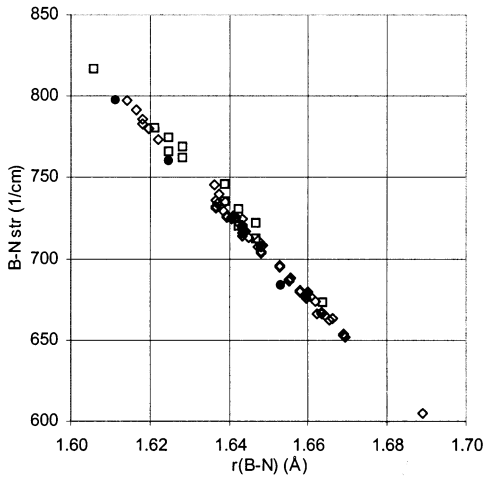

Figure 4. B−N stretching frequency, as a function of the length of this bond, for calculations on clusters **6**−**24**, using HF (diamonds) and MP2 (squares). Circular symbols represent calculations on crystals **1**, **2**, and **3**, using HF.

frequency of 773 cm^{-1}. However, it is the second least stable conglomerate of the four, after **15** and **12**.

Higher clusters will not be discussed in detail here; the reader is referred to the Supporting Information. The shortest B−N bond in the series is found for the duodecamer **23**, which is built from three S_4 **15** units; this structure gives a bond length of 1.614 Å, with an unscaled frequency of 798 cm^{-1}, for the central molecule. The general trend is that shorter bonds are found in the larger conglomerates; however, the actual value depends much on how the molecules are arranged in each system. Some calculations for selected systems at the MP2 level of theory are also given in the Supporting Information. The general trend is that, with MP2, the B−N bond is calculated to be shorter than that calculated with SCF, and the corresponding stretching frequency is higher. A graph of the B−N stretching frequency, as a function of the length of this bond, is given in Figure 4. It is clear that, over a large range, a linear relationship exists between the two calculated properties. Extrapolation to the value of 1.58 Å found experimentally in the neutron diffraction study[5] of the crystal would result in a stretching frequency of 880−900 cm^{-1}, which, after scaling, would give a value of 785−805 cm^{-1}, which is still short of the matrix results by ∼170 cm^{-1} but is in excellent agreement with the results of Taylor et al.[6−8] and Sawodny et al.[9] At smaller distances, however, the rate of the increase in the stretching frequency diminishes.

The calculations indicate that the maximum amount of bond shortening in molecular conglomerates of BH_3−NH_3 is essentially the same as that found in the crystalline state. Although individual differences are noted in the various systems, finding an arrangement of molecular dipoles that would shorten the B−N bond beyond the value found in the solid state does not appear to be possible. The variation in lengths appears to be very dependent on how the molecules are added to a specific cluster. Thus, short bonds are found in some very small clusters, e.g., the tetramer **13**, but the shortening effect is often counterbalanced by more-distant molecules in others. Hence, the results show that, although short-range interactions are an important contribution to the shortening of the B−N bond in BH_3−NH_3, the final length ultimately is determined by a balance between short- and long-range interactions.

Conclusion

Ab initio calculations were performed to investigate the effect of the crystal environment on the geometry and vibrational spectrum of borane ammoniate, BH_3−NH_3. The calculations indicate that, in the crystal, the B−N bond length shortens considerably, as confirmed by experiment. As a result of this bond shortening, the corresponding stretching frequency is calculated to change by ∼200 cm^{-1}. A reassignment of the available low-temperature matrix vibrational spectrum is proposed that unifies the available experimental data for BH_3−NH_3, in the gas phase, in solution, and in the crystalline state. Calculations on several molecular clusters show that short-range interactions are important in shortening the B−N bond, but they show that long-range interactions play an important role as well.

Acknowledgment. The authors thank Dr. C. Estherhuysen for helpful discussions.

Supporting Information Available: Text file with coordinates and vibrational frequencies of the minimized geometries of all the systems studied. This material is available free of charge via the Internet at http://pubs.acs.org.

References and Notes

(1) Thorne, L. R.; Suenram, R. D.; Lovas, F. J. *J. Chem. Phys.* **1983**, *78*, 167−171.
(2) Hughes, E. W. *J. Am. Chem. Soc.* **1956**, *78*, 502−503.
(3) Lippert, E. L.; Lipscomb, W. N. *J. Am. Chem. Soc.* **1956**, *78*, 503−504.
(4) Boese, R.; Niederprüm, N.; Bläser, D. In *Molecules in Natural Science and Medicine*−*An Encomium for Linus Pauling*; Maksić, Z. B., Eckert-Maksić, M., Eds.; Elis Horwoord: New York, 1991; pp 103−139. In this study, the B and N atoms are interchanged. A corrected refinement gives a bond length of 1.601 Å.
(5) (a) Klooster, W. T.; Koetzle, T. F.; Siegbahn, P. E. M.; Richardson, T. B.; Crabtree, R. H. *J. Am. Chem. Soc.* **1999**, *121*, 6337−6343. (b) Crabtree, R. H. *Science* **1998**, *282*, 2000−2001.
(6) Taylor, R. C.; Cluff, C. L. *Nature* **1958**, *182*, 390−391.
(7) Taylor, R. C.; Schultz, D. R.; Emery, A. R. *J. Am. Chem. Soc.* **1958**, *80*, 27−30.
(8) Taylor, R. C. *Adv. Chem. Ser.* **1964**, *42*, 59−70.
(9) Sawodny, W.; Goubeau, J. *Z. Phys. Chem.* **1965**, *44*, 227−241.
(10) Smith, J.; Seshadri, K. S.; White, D. *J. Mol. Spectrosc.* **1973**, *45*, 327−337.
(11) Umeyama, H.; Morokuma, J. *J. Am. Chem. Soc.* **1976**, *98*, 7208−7220.
(12) Binkley, J. S.; Thorne, L. R. *J. Chem. Phys.* **1983**, *79*, 2932−2940.
(13) Bühl, M.; Steinke, T.; v. R. Schleyer, P.; Boese, R. *Angew. Chem., Int. Ed. Engl.* **1991**, *30*, 1160−1161.
(14) Jiao, H.; Schleyer, P. v. R. *J. Am. Chem. Soc.* **1994**, *116*, 7429−7430.
(15) Jonas, V.; Frenking, G.; Reetz, M. T. *J. Am. Chem. Soc.* **1994**, *116*, 8741−8753.
(16) Branchadell, V.; Sbai, A.; Oliva, A. *J. Phys. Chem.* **1995**, *99*, 6472−6476.
(17) Vijay, A.; Sathyanarayana, D. N. *Chem. Phys.* **1995**, *198*, 345−352.
(18) Leboeuf, M.; Russo, N.; Salahub, D. R.; Toscano, M. *J. Chem. Phys.* **1995**, *103*, 7408−7413.
(19) Skancke, A.; Skancke, P. N. *J. Phys. Chem.* **1996**, *100*, 15079−15082.
(20) Rablen, P. R. *J. Am. Chem. Soc.* **1997**, *119*, 8350−8360.
(21) Popelier, P. L. A. *J. Phys. Chem. A* **1998**, *102*, 1873−1878.
(22) Jagielska, A.; Moszyński; R.; Piela, L. *J. Chem. Phys.* **1999**, *110*, 947−954.
(23) Kulkarni, S. A. *J. Phys. Chem. A* **1999**, *103*, 9330−9335.
(24) Frisch, M. J.; Trucks, G. W.; Schlegel, H. B.; Scuseria, G. E.; Robb, M. A.; Cheeseman, J. R.; Zakrzewski, V. G.; Montgomery, J. A., Jr.; Stratmann, R. E.; Burant, J. C.; Dapprich, S.; Millam, J. M.; Daniels, A. D.; Kudin, K. N.; Strain, M. C.; Farkas, O.; Tomasi, J.; Barone, V.; Cossi, M.; Cammi, R.; Mennucci, B.; Pomelli, C.; Adamo, C.; Clifford, S.; Ochterski, J.; Petersson, G. A.; Ayala, P. Y.; Cui, Q.; Morokuma, K.; Malick, D. K.; Rabuck, A. D.; Raghavachari, K.; Foresman, J. B.; Cioslowski, J.; Ortiz, J. V.; Stefanov, B. B.; Liu, G.; Liashenko, A.; Piskorz, P.; Komaromi, I.; Gomperts, R.; Martin, R. L.; Fox, D. J.; Keith, T.; Al-Laham, M. A.;

Peng, C. Y.; Nanayakkara, A.; Gonzalez, C.; Challacombe, M.; Gill, P. M. W.; Johnson, B. G.; Chen, W.; Wong, M. W.; Andres, J. L.; Head-Gordon, M.; Replogle, E. S.; Pople, J. A. *Gaussian 98*, revision A.7; Gaussian, Inc.: Pittsburgh, PA, 1998.

(25) Dillen, J. *QCPE Bull.* **1993**, *13*, 6.

(26) Bader, R. F. W. *Atoms in Molecules. A Quantum Theory*; Oxford University Press: Oxford, U.K., 1990.

(27) Foresman, J. B.; Frisch, Æ. *Exploring Chemistry with Electronic Structure Methods*, 2nd ed.; Gaussian, Inc.: Pittsburgh, PA, 1996.

(28) Barnes, A. J.; Hallam, H. E.; Scrimshaw, G. F. *Trans. Faraday Soc.* **1969**, *65*, 3159−3172.

(29) Penner, G. H.; Chang, Y. C.; Hutzal, J. *Inorg. Chem.* **1999**, *38*, 2868−2873.

(30) (a) Onsager, L. *J. Am. Chem. Soc.* **1936**, *58*, 1486−1493. (b) Kirkwood, J. G. *J. Chem. Phys.* **1934**, *2*, 351−361. (c) Wong, M. W.; Frisch, M. J.; Wiberg, K. B. *J. Am. Chem. Soc.* **1991**, *113*, 4776−4782. (d) Wong, M. W.; Wiberg, K. B.; Frisch, M. J. *J. Am. Chem. Soc.* **1992**, *114*, 523−529. (e) Wong, M. W.; Wiberg, K. B.; Frisch, M. J. *J. Chem. Phys.* **1991**, *95*, 8991−8998. (f) Wong, M. W.; Wiberg, K. B.; Frisch, M. J. *J. Am. Chem. Soc.* **1992**, *114*, 1645−1652.

(31) (a) Miertus, S.; Scrocco, E.; Tomasi, J. *Chem. Phys.* **1981**, *55*, 117−119. (b) Miertus, S.; Tomasi, J. *Chem. Phys.* **1982**, *65*, 239−245. (c) Cossi, M.; Barone, V.; Cammi, R.; Tomasi, J. *Chem. Phys. Lett.* **1996**, *255*, 327−335.

(32) *Handbook of Chemistry and Physics*, 82nd ed.; Lide, D. R., Ed.; CRC Press: Boca Raton, FL, 2001; Section 6, pp 151−173.

(33) Amey, R. L.; Cole, R. H. *J. Chem. Phys.* **1964**, *40*, 146−148.

(34) Richardson, T. B.; de Gala, S.; Crabtree, R. H.; Siegbahn, P. E. M. *J. Am. Chem. Soc.* **1995**, *117*, 12875−12876.